

# Theoretical study of the three-phase contact line and its tension in adsorbed colloid-polymer mixtures

Yves Vandecastel<sup>a)</sup> and Joseph O. Indekeu*Instituut voor Theoretische Fysica, Katholieke Universiteit Leuven, Celestijnenlaan 200D, B-3001 Leuven, Belgium*

(Received 14 November 2007; accepted 7 January 2008; published online 11 March 2008)

We perform a theoretical study of the three-phase contact line and the line tension in an adsorbed colloid-polymer mixture near a first-order wetting transition, employing an interface displacement model. We use a simple free-energy functional to describe a colloid-polymer mixture near a hard wall. The bulk phase behavior and the substrate-adsorbate interaction are modeled by the free-volume theory for ideal polymers. The large size of the colloidal particles and the suppression of the van der Waals interaction by optical matching of colloid and solvent justify the planar hard wall model for the substrate. Following the Fisher–Jin scheme, we derive from the free-energy functional an interface potential  $V(\ell)$  for these mixtures. For a particle diameter of 10–100 nm, the calculations indicate a line tension  $\tau \approx 10^{-12} - 10^{-13}$  N at room temperature. In view of the ultralow interfacial tension in colloid-polymer mixtures,  $\gamma \approx 10^{-7}$  N/m, this leads to a rather large characteristic length scale  $\tau/\gamma$  in the micrometer range for the three-phase contact zone width. In contrast with molecular fluids, this zone could be studied directly with optical techniques such as confocal scanning laser microscopy. © 2008 American Institute of Physics.

[DOI: 10.1063/1.2838183]

## I. INTRODUCTION

The three-phase contact line is the region where three immiscible coexisting phases meet, unless one of them wets the interface between the other two.<sup>1</sup> The excess free energy per unit length attributed to this linear inhomogeneity is called the line tension. It can be of either sign and it displays intriguing singular behavior near wetting phase transitions.<sup>2</sup>

We present the first results of a theoretical study of the three-phase contact line and its tension in a model colloid-polymer mixture in contact with a planar hard wall,<sup>3</sup> employing an interface displacement model.<sup>4</sup> Here the three phases are colloidal liquid (a phase rich in colloids and poor in polymers), colloidal gas (rich in polymers and poor in colloids), and a glass wall. The latter substrate is merely a spectator phase, in mechanical equilibrium with the adsorbate so that Young's law is applicable at three-phase contact. Wijting *et al.*<sup>5,6</sup> already reported experimental data pointing to a first-order wetting transition in colloid-polymer mixtures, although more detailed experimental evidence is called for.<sup>7,8</sup>

Away from wetting transitions and bulk critical points the line tension scales roughly as  $\tau \approx \gamma \xi$ ,<sup>1,2</sup> with interfacial tension  $\gamma \approx kT/\sigma_c^2$  and bulk correlation length, or interface thickness,  $\xi \geq \sigma_c$ , with  $\sigma_c$  the colloidal diameter. Thus one expects a line tension of the order of  $10^{-12} - 10^{-13}$  N for a particle diameter of 10–100 nm. Interestingly, these line tension magnitudes are not much smaller than those found for molecular fluids<sup>9,10</sup> due to a partial compensation of ultralow  $\gamma$  and large  $\xi$  in the colloidal system. One should bear in mind that an estimate of this type can say nothing about the sign of  $\tau$ .

This paper is organized as follows. We start from a simple density functional that describes a model colloid-polymer mixture near a hard wall.<sup>11</sup> To model the colloid-polymer mixture, we use the free-volume theory<sup>12,13</sup> (FVT) and assume ideal polymers. We then compute the interface potential from the density functional following the Fisher–Jin scheme.<sup>14</sup> The interface displacement model is employed to calculate the line tension and the interface displacement profile.

## II. SURFACE FREE ENERGY

The starting point of our analysis is the surface free-energy functional<sup>11</sup>

$$\gamma[\rho] = \int_0^\infty dz \left( f(\rho) - \mu_c \rho(z) + p_c + m(\rho) \left( \frac{d\rho}{dz} \right)^2 \right) - h_1 \rho_1 - \frac{1}{2} g \rho_1^2, \quad (1)$$

which describes an adsorbate near a hard wall. In here,  $\rho(z)$  is the order parameter profile with  $z$  the perpendicular distance to the hard wall, located at  $z = -\sigma_c/2$ . The order parameter  $\rho$  is the *colloid* number density. Since the colloid core as well as the wall are impenetrable, we have  $\rho(z) = 0$  for  $z < 0$ . A mean-field approach is adopted, in which the  $x$ - and  $y$ -dependences of  $\rho$  are neglected. We remark that it is not necessary to invoke a second independent density associated with the *polymer*, since in FVT the latter depends on  $\rho$  and on the (fixed) polymer chemical potential. This implies a considerable simplification of the computations.

The functional  $\gamma[\rho]$  consists of three parts: The first part of the integral is the contribution to the excess free energy

<sup>a)</sup>Electronic mail: yves.vandecastel@fys.kuleuven.be.

per unit area from the pressure excess  $p_c - p(z)$ , where  $p(z) \equiv \mu_c \rho(z) - f(\rho)$ , with  $f(\rho)$  the bulk free-energy density of a homogeneous fluid of uniform density  $\rho$ . The quantities  $\mu_c$  and  $p_c$  are the colloid chemical potential and pressure at two-phase coexistence of liquid and gas, respectively. It follows that the pressure excess vanishes in the coexisting bulk phases.

The second part in the integrand,  $m(\rho)(d\rho/dz)^2$ , is the leading term in an expansion in density inhomogeneities.<sup>15</sup> The coefficient of the squared gradient term is given by  $m(\rho) = (\pi/3) \int_0^\infty dr r^4 c(r, \rho)$ , where  $c(r, \rho)$  represents the direct correlation function of Ornstein and Zernike with colloid center-to-center distance  $r$  and density  $\rho$ . We will approximate the direct correlation function by<sup>16,17</sup>

$$c(r, \rho) = \begin{cases} 0, & r \leq \sigma, \\ -\beta u(r), & r > \sigma, \end{cases} \quad (2)$$

where  $u(r)$  is an attractive pairwise potential,  $\sigma$  the particle diameter, and  $\beta = 1/kT$ . This further simplifies calculations because it turns the coefficient  $m(\rho)$  into a constant  $m$ . Finally, the terms outside the integral reflect the contact interaction with the hard wall. Here  $\rho_1 \equiv \rho(0)$  is the contact density,  $h_1$  the surface field, and  $g$  the surface enhancement.<sup>11</sup>

In order to concretize the free-energy density contained in  $\gamma[\rho]$  to a model colloid-polymer mixture where the colloids and polymers have a particle diameter  $\sigma_c$  and  $\sigma_p$ , respectively, we use FVT and apply it to ideal polymers (mutually penetrable hard spheres).<sup>3,11</sup> The Helmholtz free-energy density of the homogeneous phase is then given by

$$\frac{\pi \sigma_c^3}{6kT} f(\rho) = \frac{\phi^2(4-3\phi)}{(1-\phi)^2} - \phi + \phi \ln \phi \tilde{\Lambda}_c^3 - \alpha(\phi) \phi_p^r / q^3. \quad (3)$$

Here the colloidal packing fraction is  $\phi = (\pi/6) \sigma_c^3 \rho$  and  $\phi_p^r$  is the polymer reservoir packing fraction. The size ratio is  $q = 2R_g/\sigma_c$ , with  $R_g$  the polymer radius of gyration. Further, for colloids of mass  $m_c$ ,  $\tilde{\Lambda}_c = (\pi \sigma_c^3/6)^{-1/3} (h^2/2\pi m_c kT)^{1/2}$  is the dimensionless thermal wavelength and  $\alpha(\phi)$  the averaged free-volume fraction in the unperturbed colloidal system ( $\phi_p^r = 0$ ) for which an approximate expression from the scaled particle theory can be found.<sup>18</sup> The pairwise interaction potential  $u(r)$  corresponds to the Asakura-Oosawa depletion potential,<sup>19,20</sup> the attractive part of which is given by

$$u_{AO}(r) = -kT \phi_p^r \frac{(1+q)^3}{q^3} \left( 1 - \frac{3r}{2(1+q)\sigma_c} + \frac{r^3}{2(1+q)^3 \sigma_c^3} \right) \quad (4)$$

within the range  $\sigma_c < r < \sigma_c + \sigma_p$  and which is the two-colloidal-particle interaction in a "sea" of ideal polymers.<sup>18</sup> It arises solely from the overlap of depletion zones around colloids from which polymers are excluded. The thickness of the depletion zone,  $\sigma_p/2$ , is close to, but, in general, not equal to, the polymer radius of gyration  $R_g$ . We will henceforth neglect this distinction and assume  $\sigma_p = 2R_g$ .

In the contact energy part of  $\gamma[\rho]$ , the surface field  $h_1$ , reflects the attractive colloid-wall interaction and the surface enhancement  $g$  pertains to the wall-induced correction term to the pairwise colloid-colloid interaction, which is reduced

near the wall.<sup>21</sup> In the free-volume theory for ideal polymers,  $h_1 = -\int_0^\infty dz U_2(z)$  and  $g = \int_0^\infty dz \int d\mathbf{r} U_3(z, \mathbf{r})$ .<sup>3,11</sup> Here  $U_2$  is the gain in free volume accessible for polymers when one colloid approaches the hard wall.  $U_3$  is the triple-overlap volume of the depletion zones of two colloids and the planar hard wall, which is counted three times [once in  $u(r)$  and twice in  $U_2$ ], but should only be counted twice. In other words, any part of an excluded zone belonging to a colloid can become free only once. Our working model of a colloid-polymer mixture features  $q=1$  and  $\phi_p^r=1.917$ , which brings the system near a first-order wetting transition.<sup>11</sup>

Note that the free-energy functional we employ is adequate (only) for a fluid made up of particles whose interactions are short ranged. Also the adsorbate-substrate energy is strictly local and thus short ranged as well. For molecular fluids with van der Waals forces this would be an approximation which misses a lot of the physics. However, due to refractive index matching (for the relevant frequency range) and static dielectric constant matching<sup>22</sup> of colloid and solvent, the dynamic (dispersion) and static contributions to the van der Waals forces are practically absent.<sup>23</sup> This implies that, to a good approximation, all adsorbate-adsorbate and adsorbate-substrate interactions at the level of the colloidal particles are indeed of finite range (of the order of the colloid radius augmented with the effective polymer radius). This circumstance renders the theoretical description we presently employ exceptionally adequate for the system at hand.

### III. INTERFACE POTENTIAL

The interface potential  $V(\ell)$  gives by definition the excess free energy per unit area of a homogeneous film of liquid of fixed thickness  $\ell$  adsorbed at the wall-gas interface. It is therefore to be interpreted as a constrained, and thus, in general, nonequilibrium, surface free energy. In order to obtain an interface potential  $V(\ell)$  from the functional  $\gamma[\rho]$ , a self-consistent approach is to impose a crossing constraint  $\rho(\ell) = \rho^\times$ , as proposed by Fisher and Jin.<sup>14</sup> The value of  $\rho^\times$  is arbitrary as long as it lies in between the bulk liquid and gas densities. In practice it is advantageous to choose it close enough to the gas density in order to be able to work with positive values of  $\ell$  even for small amounts of adsorbed colloid.

Minimizing  $\gamma[\rho]$  with respect to  $\rho(z)$  at fixed  $\ell$  generates the interface potential  $V(\ell)$ . To determine the family of optimal density profiles, we use the Euler-Lagrange equation in the region  $0 < z < \ell$ , subject to a wall boundary condition, and in the region  $\ell < z < \infty$ , subject to the bulk condition  $\rho(\infty) = \rho_g$ , where  $\rho_g$  is the bulk gas density. The Euler-Lagrange equation reads

$$2m \frac{d^2 \rho}{dz^2} = \frac{df(\rho)}{d\rho} - \mu_c \quad (5)$$

and the wall boundary condition is

$$-h_1 - g\rho_1 = 2m \frac{d\rho}{dz}(0). \quad (6)$$

We now describe a numerical scheme to construct the interface potential  $V(\ell)$  from  $\gamma[\rho]$ . We make use of the constant

of motion, which is the first integral of the second-order Euler–Lagrange differential equation, and has the benefit of involving only  $\rho$  and its first derivative. It is given by

$$m(dp/dz)^2 - f(\rho) + \mu_c \rho - p_c = E, \quad (7)$$

where  $E$  is a constant. In the interval  $0 < z < \ell$ ,  $E$ , in general, differs from zero since  $E$  must be adjusted in order that  $\rho(\ell) = \rho^\times$  be satisfied. For example, for a profile  $\rho(z)$  that is monotonically decreasing between the wall and  $z = \ell$  the dependence of  $\ell$  on  $E$  takes the simple form

$$\ell = \int_{\rho_1}^{\rho^\times} \frac{dz}{d\rho} d\rho = \int_{\rho_1}^{\rho^\times} d\rho \frac{\sqrt{m}}{\sqrt{E + f(\rho) - \mu_c \rho + p_c}}. \quad (8)$$

In the interval  $\ell < z < \infty$ ,  $E = 0$  because of the bulk convergence of the density profile, i.e.,  $\rho(z) \rightarrow \rho_g$  for  $z \rightarrow \infty$ . Consequently, there is typically a discontinuity in  $E$  reflecting a discontinuity in  $dp/dz$  at  $z = \ell$ , while  $\rho(z)$  is continuous. It is possible to smoothen this singularity systematically by generalizing the crossing constraint to include integral constraints.<sup>24</sup>

Evaluation of the constrained profile in the functional  $\gamma[\rho]$  leads to the excess free energy per unit area, which, up to an irrelevant additive constant, should be the interface potential  $V(\ell)$  we wish to extract. In general, however, extra care must be taken to ensure obtaining the minimal value of the constrained surface free energy for a given  $\ell$ . The reason for this is that, in general,  $V(\ell)$  is not a function but a multivalued map, as we shall now demonstrate.

It is useful to examine, for a given fixed  $\ell$ , the constrained surface free energy as a function of the wall value  $\rho_1$ . This can be done by temporarily relieving the wall boundary condition [Eq. (6)] and, instead, treating  $\rho_1$  as a control variable. We then obtain a curve which we denote by  $W_\ell(\rho_1)$  [see Fig. 1(a)]. The extrema of this curve correspond to constrained profiles which satisfy also Eq. (6). Some of these extrema are local minima; only the lowest value of the curve provides  $V(\ell)$ . For a range of values of  $\ell$  it is seen that two local minima occur, which can compete. The order parameter profiles corresponding to the extrema of  $W$  can be conveniently visualized with the help of the phase portrait method, which consists of plotting  $dp/dz$  versus  $\rho$  [see Fig. 1(b) and its caption for details]. Plotting the constrained surface free energy in the local minima of  $W$  as a function of  $\ell$  entails the multivalued map shown in Fig. 2. Finally, the lowest value of this map is the interface potential function  $V(\ell)$ .

The calculations reveal that we must distinguish *single crossing profiles*  $\rho(z)$ , which cross  $\rho^\times$  only once, and *double crossing profiles*, which are nonmonotonic and attain the value  $\rho^\times$  at two distinct distances  $z$  from the wall, the largest of which corresponds to  $z = \ell$ . Both kinds of profiles arise naturally from imposing properly the crossing constraint, and are illustrated in the phase portrait [see Fig. 1(b)]. It is not the first time that multiple crossings are encountered in the frame work of the Fisher–Jin constraint. Boulter and Clarisse met them in a different complex fluid model, but did not need them, and for convenience limited their considerations to single crossing profiles.<sup>25,26</sup> In our present context, how-

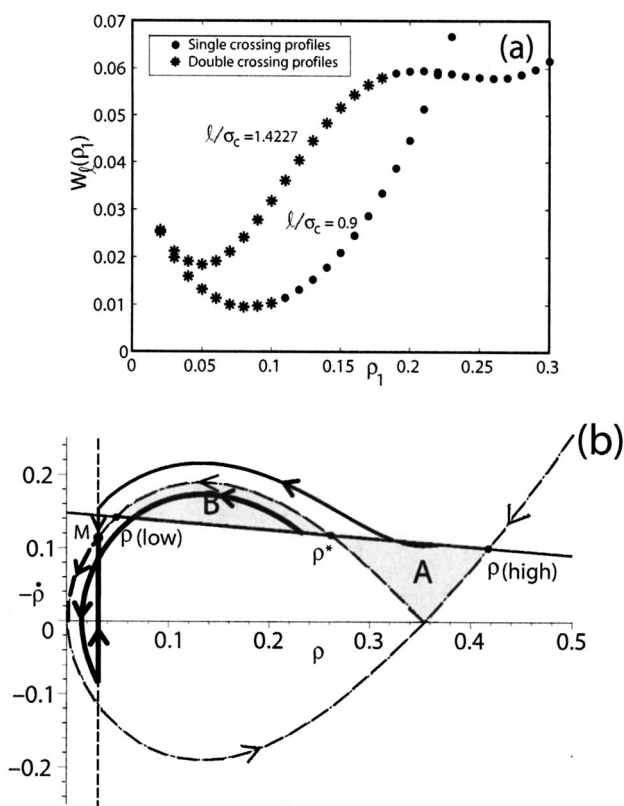


FIG. 1. (a) Constrained surface excess free energy  $W_\ell(\rho_1)$ , in units of  $kT/(\pi\sigma_c/6)^2$ , for two values of the wetting film thickness  $\ell$  as a function of the wall value  $\rho_1$  of the order parameter  $\rho$ , in units of  $1/(\pi\sigma_c^3/6)$ . Circles are for single crossing profiles and rosettes for double crossing profiles. For  $\ell/\sigma_c = 0.9$  a single minimum is apparent, while for  $\ell/\sigma_c = 1.4227$  two competing (local) minima and one maximum are found. (b) Phase portrait,  $dp/dz$ , in units of  $1/(\pi\sigma_c^4/6)$ , vs  $\rho$ , with trajectories for smooth and constrained profiles. The bulk liquid and gas densities are at  $\rho_l = 0.354$  and  $\rho_g = 0.773 \times 10^{-4}$ , and the crossing density is at  $\rho^\times = 0.03$ . Smooth (unconstrained) profiles are characterized by  $E = 0$  and follow the thin dashed-dotted trajectories (with arrows) leading to the fixed points at the bulk densities. The wall boundary condition is satisfied at intersections of the (almost) horizontal straight line with the trajectories. Solutions starting at  $\rho_1 = \rho(\text{low})$ ,  $\rho^*$ , and  $\rho(\text{high})$  correspond to thin film minimum, saddle point, and wetting layer minimum in the surface free energy, respectively. At first-order wetting areas A and B are equal. Constrained profiles follow the thicker and solid trajectories (with arrows), which display a jump in  $dp/dz$  at  $\rho^\times$  (vertical dashed line) toward point M, before joining the thick dashed trajectory going into the gas fixed point, near the origin. A single-crossing profile (top trajectory; medium thick solid line) passes the crossing density only once, while a double crossing profile (innermost trajectory; thickest solid line) first passes  $\rho^\times$  smoothly, then returns to  $\rho^\times$  and jumps up to point M. Incidentally, fixing  $\ell/\sigma_c \approx 1.4227$  [see Fig. 1(a)] and imposing the wall boundary condition reproduces the smooth profile with contact density  $\rho_1 = \rho^*$ .

ever, a similar limitation would be mathematically inconsistent and lead to a severely incomplete and useless interface potential.

The interface potential we obtain displays a parabolic minimum at small  $\ell$  and an exponentially rapid descent toward another minimum for  $\ell \rightarrow \infty$ , separated by a maximum at intermediate  $\ell$ . At a first-order wetting phase transition, for model parameters very close to the ones we have adopted in the calculations, the two minima are equal in surface free energy and represent a thin adsorbed film coexisting with a macroscopic wetting layer. The values of  $V(\ell)$  in the vicinity



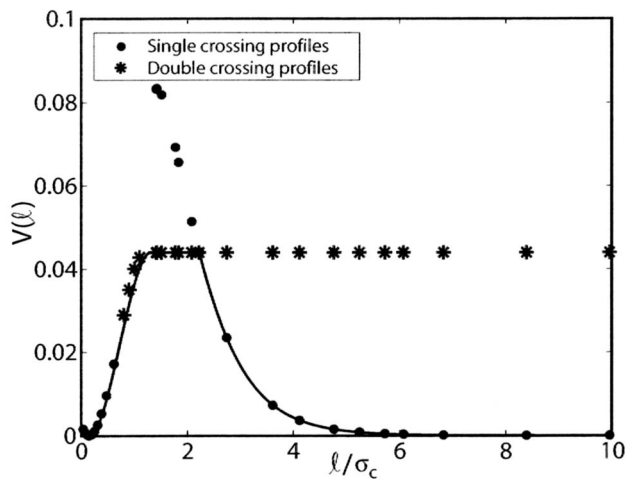


FIG. 2. The interface potential  $V(\ell)$  for our model colloid-polymer mixture at a first-order wetting transition, in units of  $kT/(\pi\sigma_c/6)^2$ , obtained by a fit through the minimal surface free energy values for profiles computed using the Fisher–Jin crossing constraint. Circles denote values for single crossing profiles, rosettes correspond to double crossing profiles.

of these minima correspond to order parameter profiles which are close to the equilibrium solutions of the variational problem without constraint. For these solutions the contact densities  $\rho_1 = \rho$  (low adsorption) and  $\rho_1 = \rho$  (high adsorption) satisfy the wall boundary condition [Eq. (6)],

$$h_1 + g\rho_1 = 2\sqrt{m(f(\rho_1) - \mu_c\rho_1 + p_c)}, \quad (9)$$

and the density profiles are everywhere smooth [see Fig. 1(b)].

For  $\ell/\sigma_c > 1.4$  two local surface free-energy minima in  $W_\ell(\rho_1)$  appear [see Fig. 1(a)]. In the interval  $\ell/\sigma_c \in [1.4, 2.22]$ , the minimum of  $W$  for single crossing profiles is higher than that for double crossing profiles. This ordering must at some point be reversed because it is easy to estimate that for large  $\ell$  the latter must converge to a constant higher than the value of the former. Indeed, at  $\ell/\sigma_c \approx 2.22$ , the two minima in  $W_\ell(\rho_1)$  exchange stability. This leads to a discontinuity in the derivative of the minimal value, i.e., the function  $V(\ell)$ .

Our numerical results are well fitted by the following piecewise analytic expression for the  $V(\ell)$ ,

$$V(\ell) = \begin{cases} a_2(\ell - \ell_0)^2 + a_3(\ell - \ell_0)^3, & 0 < \ell < \ell_1, \\ c_0, & \ell_1 < \ell < \ell_2, \\ b_1e^{-\ell/\xi} + b_2e^{-2\ell/\xi} + b_0, & \ell_2 < \ell. \end{cases} \quad (10)$$

In Fig. 2 this function is drawn (smooth lines) for the parameter values  $a_2 = 0.0977$ ,  $a_3 = -0.05607$ ,  $b_0 = 0.00004$ ,  $b_1 = 1.21375$ ,  $b_2 = -4.73153$  and  $c_0 = 0.04394$ , in units of  $kT/(\pi\sigma_c/6)^2$ , and  $\xi = 0.70941$ ,  $\ell_0 = 0.1468$ ,  $\ell_1 = 1.3084$ ,  $\ell_2 = 2.2220$ , in units of  $\sigma_c$ . The values of  $\ell_1$  and  $a_3$  have been chosen so as to connect smoothly the first two segments. We determined the very small value  $b_0 = \lim_{\ell \rightarrow \infty} V(\ell)$  from the spreading coefficient<sup>2</sup> which is proportional to the difference between areas A and B in Fig. 1(b). Since  $b_0$  is practically

zero, the computed  $V(\ell)$  properly describes the immediate vicinity of the first-order wetting transition.

#### IV. LINE TENSION AND INTERFACE DISPLACEMENT PROFILE

By considering the liquid and the gas phase in contact with a rigid planar hard wall in the  $xy$ -plane at  $z=0$  (more precisely,  $z = -\sigma_c/2$ ) we express the excess free energy per unit length  $\tau$  associated with a surface inhomogeneity uniform in the  $y$ -direction as a functional of the displacement  $\ell(x)$  of the interface in the  $z$ -direction,<sup>4,27</sup>

$$\tau[\ell] = \int_{-\infty}^{\infty} dx \left[ \gamma_{LG} \left( \sqrt{1 + \left( \frac{d\ell}{dx} \right)^2} - 1 \right) + V(\ell(x)) + c(x) \right], \quad (11)$$

where  $\gamma_{LG}$  is the liquid-gas interfacial tension,  $V(\ell)$  is the interface potential and the piecewise constant  $c(x)$  must be chosen so as to make the integrand of  $\tau[\ell]$  tend to zero at large values of  $|x|$ , away from the surface inhomogeneity.<sup>4</sup> In the often used squared gradient approximation,  $\sqrt{1 + (d\ell/dx)^2} \approx 1 + (1/2)(d\ell/dx)^2$ , applied to  $\tau[\ell]$ , the line tension  $\tau$ , which minimizes the functional, is given by<sup>4</sup>

$$\tau = (2\gamma_{LG})^{1/2} \int_{\ell_1}^{\infty} d\tilde{\ell} [V(\tilde{\ell})^{1/2} - E^{1/2}], \quad (12)$$

where  $\tilde{\ell} = \ell/\xi$ ,  $\ell_1$  is the film thickness at the thin film minimum, and  $\lim_{\ell \rightarrow \infty} V(\ell) = E$ . For the model colloid-polymer mixture studied here, we obtain from Eq. (12) a positive line tension  $\tau = 1.3 \times 10^{-20} \text{ J}/\sigma_c \approx 10^{-12} - 10^{-13} \text{ N}$  at room temperature, for colloidal diameter of 10–100 nm, respectively. We calculated the value of the interfacial tension  $\gamma_{LG} = 1.412 \times 10^{-20} \text{ J}/\sigma_c^2 \approx 10^{-4} - 10^{-6} \text{ N/m}$  from the standard squared gradient functional of the fluid-fluid interface (see also Refs. 11 and 29). The width of the three-phase contact zone  $\tau/\gamma_{LG}$  scales with the particle diameter, implying that the three-phase contact zone should be observable directly with optical techniques such as confocal laser scanning microscopy. Using Eq. (11), we remark that the theory predicts a contact zone width in the range of at least 50  $\mu\text{m}$  from the calculated interface displacement profile near first-order wetting (see Fig. 3).

#### V. CONCLUSIONS

From a simple free-energy functional that models a colloid-polymer mixture near a planar hard wall, we calculated an interface potential near a first-order wetting transition following the Fisher–Jin scheme. In this free-energy functional, we used as a starting theory to describe the mixture the free-volume theory for ideal polymers. The calculations of the line tension  $\tau$ , which is theoretically predicted to reach a positive (local) maximal value at a first-order wetting transition, yield an estimate of  $10^{-12} \text{ N}$  which is not much smaller than typical absolute values of line tensions that have been reported for molecular fluids.<sup>28,29</sup> The ultralow interfacial tension in colloid-polymer mixtures leads to a character-

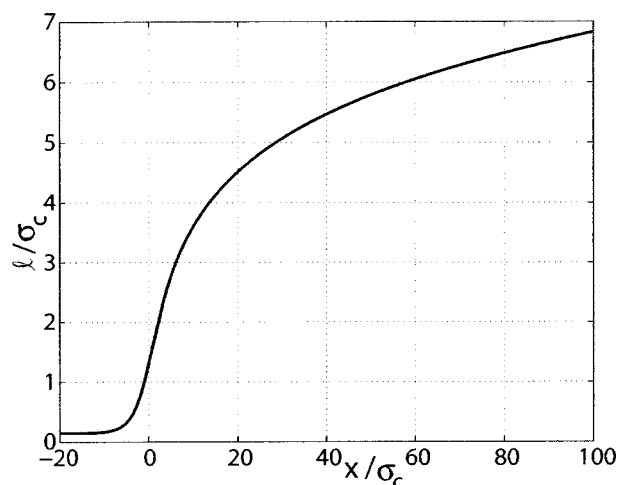


FIG. 3. Calculated interface displacement profile  $\ell(x)$  for our model colloid-polymer mixture at a first-order wetting transition, using the analytic approximations to  $V(\ell)$ . The liquid (gas) is situated below (above) the interface (solid line). The substrate surface runs along the horizontal axis. There are two (imperceptible) singularities in the profile, at  $\ell = \ell_1$  and  $\ell = \ell_2$ . For large  $x$ ,  $\ell$  increases as  $\log(x)$  (see Ref. 4).

istic width in the optical wavelength range for the three-phase contact zone, whereas in molecular fluids the range is of the order of Ångströms. Our calculation of the interface displacement profile near the first-order wetting transition predicts an extended three-phase contact zone in the range of at least 50 colloidal diameters.

Further theoretical challenges include making the polymers more realistic and examining the size ratio and polymer fugacity dependence of the line tension and the interface displacement profiles. It should be of interest as well to compare the results of the interface displacement model with more quantitative density functional studies of the line tension,<sup>30</sup> and with experimental data.

## ACKNOWLEDGMENTS

We are much indebted to Dirk Aarts for discussions. This research is supported by FWO-Vlaanderen, Project No. G.0483.04.

- <sup>1</sup>J. S. Rowlinson and B. Widom, *Molecular Theory of Capillarity* (Clarendon, Oxford, 1989); L. Schimmele, M. Napiórkowski, and S. Dietrich, *J. Chem. Phys.* **127**, 164715 (2007).
- <sup>2</sup>J. O. Indekeu, *Int. J. Mod. Phys. B* **8**, 309 (1994).
- <sup>3</sup>D. G. A. L. Aarts, "The interface in demixed colloid-polymer systems," Ph.D. thesis, University of Utrecht, 2005.
- <sup>4</sup>J. O. Indekeu, *Physica A* **183**, 439 (1992).
- <sup>5</sup>W. K. Wijting, N. A. M. Besseling, and M. A. Cohen Stuart, *Phys. Rev. Lett.* **90**, 196101 (2003).
- <sup>6</sup>W. K. Wijting, N. A. M. Besseling, and M. A. Cohen Stuart, *J. Phys. Chem. B* **107**, 10565 (2003).
- <sup>7</sup>D. G. A. L. Aarts and H. N. W. Lekkerkerker, *J. Phys.: Condens. Matter* **16**, S4231 (2004).
- <sup>8</sup>D. G. A. L. Aarts, J. H. van der Wiel, and H. N. W. Lekkerkerker, *J. Phys.: Condens. Matter* **15**, S245 (2003).
- <sup>9</sup>S. Herminghaus and T. Pompe, *Phys. Rev. Lett.* **85**, 85 (2000).
- <sup>10</sup>T. Pompe, *Phys. Rev. Lett.* **89**, 076102 (2000).
- <sup>11</sup>D. G. A. L. Aarts, R. P. A. Dullens, H. N. W. Lekkerkerker, D. Bonn, and R. van Roij, *J. Chem. Phys.* **120**, 1973 (2004).
- <sup>12</sup>H. N. W. Lekkerkerker, *Colloids Surf.* **51**, 419 (1990).
- <sup>13</sup>H. N. W. Lekkerkerker, W. C. K. Poon, P. N. Pusey, A. Stroobants, and P. B. Warren, *Europhys. Lett.* **20**, 559 (1992).
- <sup>14</sup>M. E. Fisher and A. J. Jin, *Phys. Rev. B* **44**, 1430 (1991).
- <sup>15</sup>R. Evans, *Adv. Phys.* **28**, 143 (1979).
- <sup>16</sup>J. M. Brader and R. Evans, *Europhys. Lett.* **49**, 678 (2000).
- <sup>17</sup>J.-P. Hansen and I. R. McDonalds, *Theory of Simple Liquids*, 2nd ed. (Academic, London, 1990).
- <sup>18</sup>M. Dijkstra, R. van Roij, and R. Evans, *Phys. Rev. Lett.* **81**, 2268 (1998).
- <sup>19</sup>S. Asakura and F. Oosawa, *J. Chem. Phys.* **22**, 1255 (1954).
- <sup>20</sup>A. Vrij, *Pure Appl. Chem.* **48**, 471 (1976).
- <sup>21</sup>Strictly speaking, the surface field is the coefficient of  $\rho_1 - \rho_c$  and the surface enhancement that of  $(\rho_1 - \rho_c)^2$ , where  $\rho_c$  is the bulk colloid density at the liquid-gas critical point. Note also that in our definition  $g$  is minus  $g$  in Ref. 11.
- <sup>22</sup>For example, the static dielectric constants of poly-methylmethacrylate (PMMA) (colloids) and decaline (solvent) are about 2.6 and 2.2, respectively, which leads to a weak interaction of order  $0.01kT$  only. Further, measurement confirms that under these circumstances PMMA colloids interact like hard spheres; D. Aarts, personal communication (2007).
- <sup>23</sup>J. N. Israelachvili, *Intermolecular and Surface Forces* (Academic, London, 1992).
- <sup>24</sup>C. J. Boulter and J. O. Indekeu, *Phys. Rev. E* **56**, 5734 (1997).
- <sup>25</sup>C. J. Boulter and F. Clarysse, *Phys. Rev. E* **60**, R2472 (1999).
- <sup>26</sup>F. Clarysse and C. J. Boulter, *Physica A* **278**, 356 (2000).
- <sup>27</sup>H. T. Dobbs and J. O. Indekeu, *Physica A* **201**, 457 (1993).
- <sup>28</sup>A. Amirfazli and A. W. Neumann, *Adv. Colloid Interface Sci.* **110**, 121 (2004).
- <sup>29</sup>J. Drelich, *Colloids Surf., A* **116**, 43 (1996).
- <sup>30</sup>C. Bauer and S. Dietrich, *Eur. Phys. J. B* **10**, 767 (1999).